JOC The Journal of Organic Chemistry

Article

pubs.acs.org/joc

Tetraphenylethene−2-Pyrone Conjugate: Aggregation-Induced Emission Study and Explosives Sensor

Vaithiyanathan Mahendran,[†] Kamaraj Pasumpon,[†] Solaimalai Thimmarayaperumal,[†] Pakkirisamy Thilagar,[‡] and Sivakumar Shanmugam*[,†]

[†]Department of Organic Chemistry, School of Chemistry, Madurai Kamaraj University, Madurai 625 021, India

[‡]Department of Inorganic and Physical Chemistry, Indian Institute of Science, Bangalore 560 012, India

Supporting Information

ABSTRACT: Design and synthesis of a novel tetraphenylethene−2-pyrone (**TPEP**) conjugate exhibiting donor−acceptor characteristics is reported. The localized frontier molecular orbitals (DFT studies) and the solvent polarity dependent photoluminescence characteristics directly corroborate the presence of intramolecular charge transfer character in **TPEP**. **TPEP** is poorly emissive in the solution state. In contrast, upon aggregation (THF/water mixtures), **TPEP** exhibits aggregation-induced emission enhancement. Upon aggregation, dyad **TPEP** forms a fluorescent nanoaggregate which was confirmed by transmission electron microscopy imaging studies. The luminescence nanoaggregates were elegantly exploited for selective detection of nitro aromatic compounds (NACs). It was found that nanoaggregates of **TPEP** were selectively sensing the picric acid over the other NACs. Efficiency of the quenching process was further evaluated by the Stern−Volmer equation. **TPEP**-based low-cost fluorescent test strips were developed for the selective detection of picric acid.

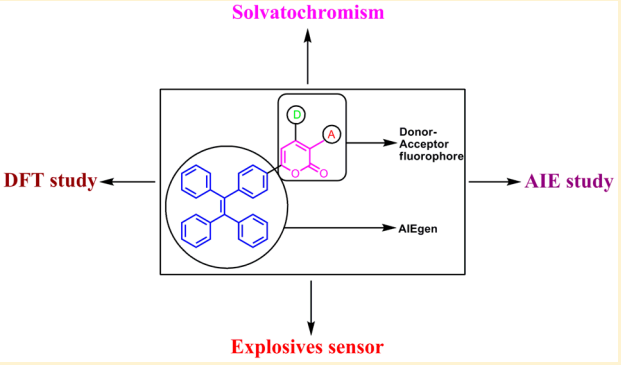

INTRODUCTION

Fluorescent organic materials have been receiving tremendous attention in the field of science and technology owing to their potential applications such as sensors,[1] bioimaging agents,[2] fluorescent probes,[3] and organic light-emitting devices (OLEDs).[4] Most of the fluorescent organic molecules are planar in nature and highly emissive in dilute solutions. The light-emitting nature of many fluorescent molecules is affected by the notorious problem called aggregation-caused quenching (ACQ). ACQ is the phenomenon by which light emission of many organic fluorescent molecules is partially or totally quenched in the aggregated/solid state. Consequently, the ACQ process affects the real time applications of a molecule under investigation. Formation of excimers through $\pi-\pi$ stacking is one of the proposed reasons for ACQ of planar fluorescent molecules by which nonradiative relaxation from the excited states has been observed. On the other hand, aggregation-induced emission[5] (AIE) was discovered by Tang et al. in 2001, and since then it has become a useful concept for designing organic molecules that are free from ACQ properties. They disclosed that the series of propeller-shaped organic molecules are nonemissive when they are molecularly dissolved in solvents and became a highly emissive in the aggregated state. Restriction of intramolecular motion[6] (RIM) was the proposed mechanism for the AIE property of any molecule. After discovery of the AIE phenomenon, numerous research groups have been enthusiastically devoting their research efforts for the design and development of novel AIE active molecules. The potential applications AIE luminogens have been well documented in recent literature.[7]

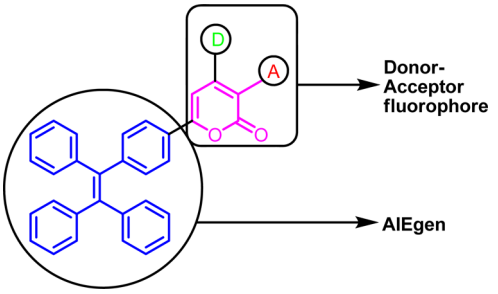

Figure 1. Design of **TPEP**.

It was reported that one can rationally design and change the ACQ nature of a fluorophore into the AIE-active fluorescent molecule by incorporating typical AIE active luminogen (AIEgen) to the molecular structure of the fluorophore.[8] Tetraphenylethene[9] (TPE) is one among such AIE-active luminogens, and 2-pyrone (2*H*-pyran-2-one) is a fluorophore that has shown interesting electroluminescence properties and

Received: February 5, 2016
Published: April 6, 2016

DOI: 10.1021/acs.joc.6b00267
J. Org. Chem. 2016, 81, 3597−3602

Scheme 1. Synthetic Route to TPEP

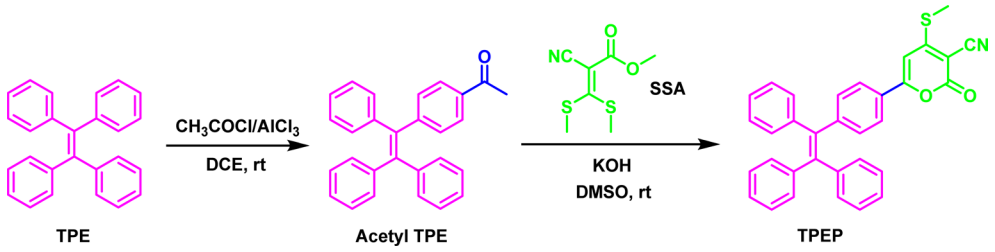

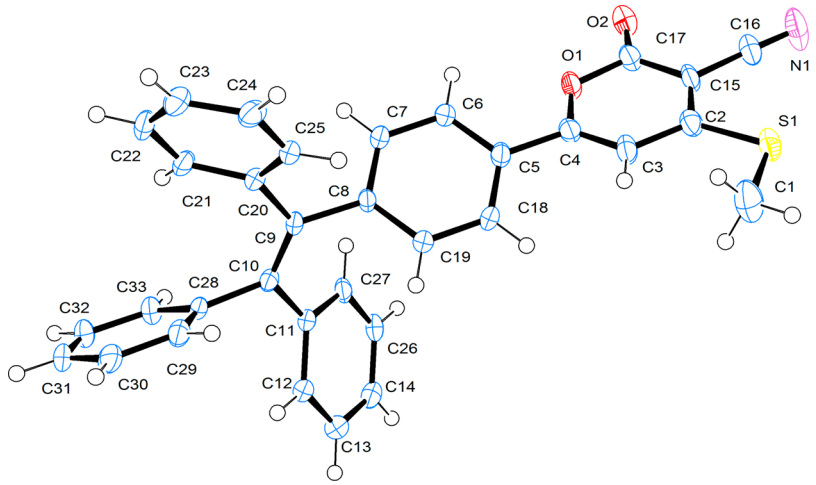

Figure 2. Molecular structure of **TPEP** (carbon, blue; hydrogen, white; nitrogen, pink; oxygen, red; sulfur, yellow).Thermal ellipsoids are at a 50% probability level.

found applications in OLED.[10] We recently became interested in the design and development of novel AIE-active luminogens for selective detection and discrimination of nitroaromatic-based explosives.[11] As part of our ongoing program, we investigated the structure and AIE characteristics of a novel donor–acceptor (D–A) system containing TPE and 2-pyrone moieties (**TPEP**, Figure 1). Compound **TPEP** forms fluorescence nanoaggregates in the aggregated state and selectively detects picric acid and discriminates against other nitroaromatic compounds (NACs). The intriguing optical properties of **TPEP** are reported in this manuscript.

RESULTS AND DISCUSSION

Compound **TPEP** was synthesized according to the synthetic procedure shown in Scheme 1. The base-mediated reaction between **acetyl TPE** and **SSA** in DMSO solvent yielded **TPEP** in decent yield. Compound **TPEP** was well characterized by ^{1}H, ^{13}C NMR and HRMS analysis. The molecular structure of **TPEP** was confirmed by single-crystal X-ray diffraction studies (Figure 2). Single crystals of **TPEP** were obtained by slow evaporation of solutions of **TPEP** in 1:1 solvent mixtures of chloroform and methanol. Compound **TPEP** crystallized in the triclinic crystal system with the $P\bar{1}$ space group (Supporting Information). From the crystal structure, it was found that the **TPEP** unit adopted a twisted molecular confirmation as observed in numerous reported TPE-derived molecules.

Compound **TPEP** is highly soluble in common organic solvents such as hexane, THF, chloroform, dichloromethane (DCM), and methanol (MeOH) and insoluble in water. The photophysical properties were screened using UV–vis and fluorescence spectroscopy. The UV–vis spectrum (Supporting Information) in THF (1×10^{-5} M) exhibits absorption maxima at 403 and 300 nm. The lower energy absorption was assigned to intramolecular charge transfer from TPE to the 2-pyrone part of the **TPEP** and higher energy absorption ascribed to the π–π^* transition of the TPE part of the **TPEP**. The PL spectrum in THF shows the emission maxima at 536 nm. Furthermore, the solvatochromic properties of **TPEP** were screened using various solvents with different polarity (Figure 4a). The UV–vis absorption spectra of **TPEP** in both nonpolar and polar solvents were almost similar. However, a red shift was observed in the emission spectrum when the solvent polarity was increased. This confirms the involvement of an intramolecular charge-transfer process in **TPEP**, which is typically observed in D–A systems. In hexane, emission maxima were observed at 494 nm (Stokes shift, $\Delta\nu$ = 5300 cm^{-1}), for THF and DCM, emission maxima were located at 536 nm ($\Delta\nu$ = 6600 cm^{-1}) and 572 nm ($\Delta\nu$ = 7500 cm^{-1}). On the other hand, in MeOH, emission maxima was bathochromically shifted to 600 nm ($\Delta\nu$ = 8100 cm^{-1}).

AIE Property. It is well-known that TPE-derived molecules exhibit aggregation-induced emission characteristics. The presence of the TPE unit in **TPEP** and its insoluble characteristics in water encouraged us to study the aggregation-induced emission property of **TPEP** in THF/water solvent mixtures. The absorption maxima at 403 nm of 100% THF solution of **TPEP** was red-shifted to 455 nm upon addition of 90% water with a leveling-off long-wavelength tail, confirming the formation of nanoparticles (Supporting Information). The leveling-off long-wavelength tail can be attributed to the well-known Mei scattering effect, which has been documented in the literatures for AIE-active luminogens.[12]

DOI: 10.1021/acs.joc.6b00267
J. Org. Chem. 2016, 81, 3597–3602

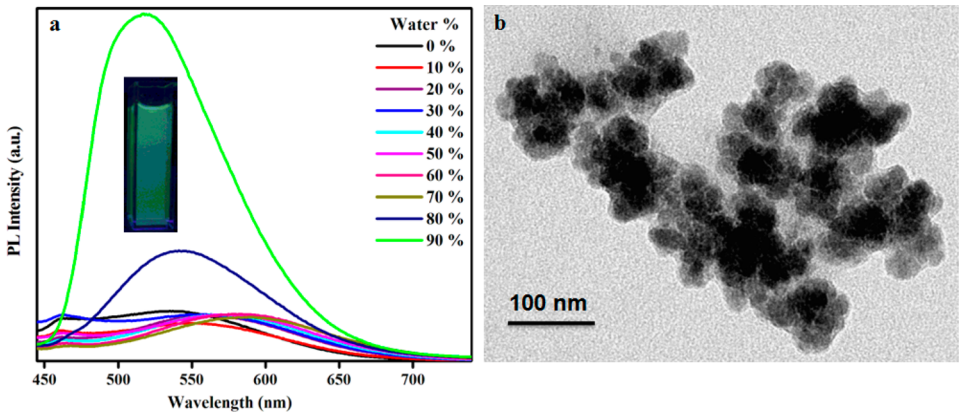

Figure 3. Emission spectra of **TPEP** in THF/water solvent mixtures (a) and TEM image of **TPEP** aggregates formed in THF/water mixture with 90% water fraction (b). Inset: photograph of the fluorescence emission of **TPEP** aggregates formed in THF/water mixture with 90% water fraction (excitation wavelength: 365 nm).

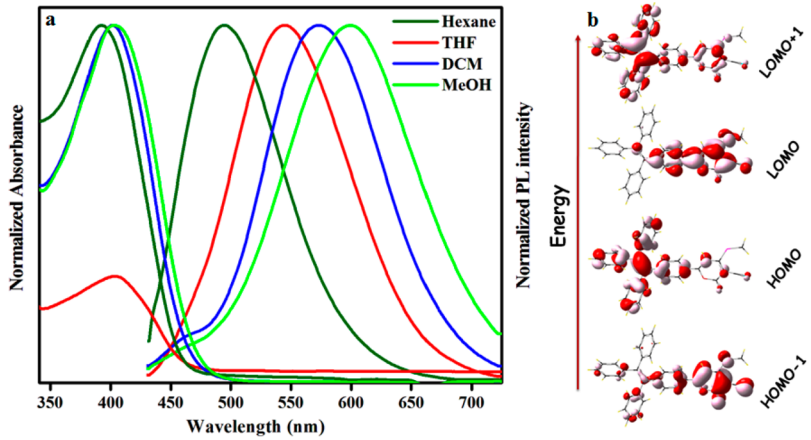

Figure 4. UV−vis and emission spectra of **TPEP** in solvents with different polarity (a) and selected frontier molecular orbitals for **TPEP** (b) (isovalue = 0.03).

The 100% THF solution of **TPEP** is weakly emissive with a λ_{max} at ∼536 nm. The photoluminescence feature of **TPEP** is insensitive (no spectral changes) to the initial addition of water fractions ∼10 and 20%. It was observed that upon addition of 30−70% of water fraction the PL spectra of **TPEP** progressively red-shifted to 585 nm without changing the emission intensity. The addition of water increases the polarity of the solvent medium, and hence, the emission of **TPEP** (with D−A structure) shifted to longer wavelength. However, at this point we do not know why the luminescent intensity is insensitive to the polarity of the solvent medium. Interestingly, at addition of 90% water fractions, the PL intensity enhanced rapidly, and the luminescence maxima were blue-shifted to 518 nm. The weak emissive characteristics of **TPEP** in dilute solutions can be attributed to the enhanced nonradiative decay due to the molecular free rotations. However, upon aggregation the molecular free rotations ceased and the photoexcited molecule prefers to relax via radiative-decay pathway. Thus, enhanced luminescence intensity was observed for **TPEP** in an aggregated state. The transmission electron microscopy (TEM) images of the aggregated samples of **TPEP** confirm the formation of nanoparticles (Figure 3b).

Theoretical Investigations. To understand the electronic structure of **TPEP**, DFT computational studies were performed. The hybrid B3LYP[13] functional has been used for all calculations as incorporated in the Gaussian 09 package[14] by mixing the Hartree−Fock-type exchange with Becke's exchange functional[15] and that developed by Lee−Yang−Parr for the correlation contribution.[16] We have considered the 6-31G(d) basis set for all of the atoms, which provides reasonably good quality results in reasonable time scales. Visualizations of the optimized structures and the MOs were performed using Gaussview5.0. The harmonic force constants were computed at the optimized geometries to characterize the stationary points as minima. TD-DFT vertical excitation calculations were performed for **TPEP** on the basis of their ground-state optimized structures.

The frontier molecular orbital of **TPEP** is shown in Figure 4b. The HOMO is mainly localized on the TPE unit with less contribution from the 2-pyrone ring, and the LUMO is mainly localized on the 2-pyrone ring with considerable contribution from the phenyl ring of the TPE unit which is attached with 2-pyrone. On the other hand, HOMO-1 is localized on the 2-pyrone ring and LUMO+1 is TPE centered with less contribution from the 2-pyrone ring. The localized frontier molecular orbitals of **TPEP** clearly indicate that molecule may redistribute the charge upon photoexcitation. This result is in agreement with the experimentally observed solvent polarity dependent PL characteristics of **TPEP**. The possible electronic transitions involved in **TPEP** were calculated using TD-DFT methods. The results revealed that the longer wavelength absorption of **TPEP** originates from HOMO to LUMO, which

DOI: 10.1021/acs.joc.6b00267
J. Org. Chem. 2016, 81, 3597−3602

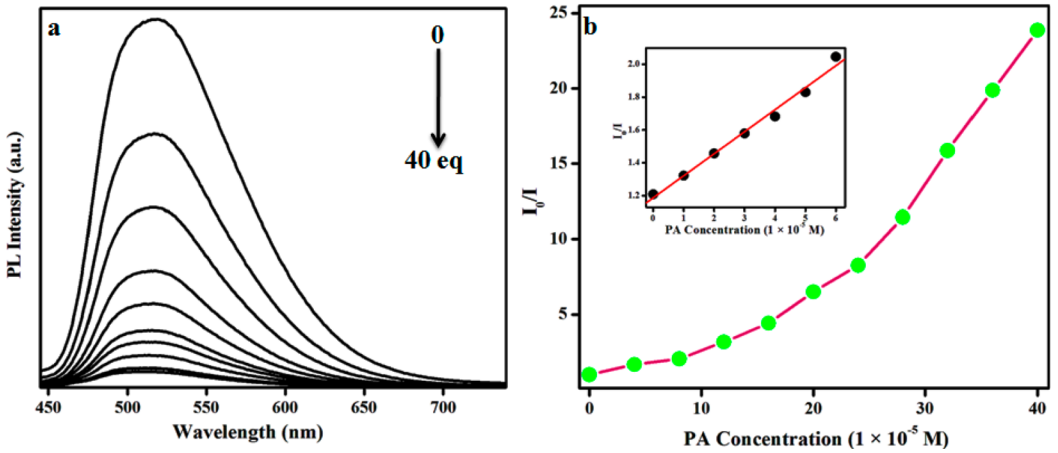

Figure 5. Change in fluorescence spectra of **TPEP** with the addition of PA in THF/water (10:90) mixtures (a), Stern–Volmer plot in response to PA (b). Inset: Stern–Volmer plot obtained at lower concentration of PA.

involve charge transition from TPE to 2-pyrone and higher energy absorption of **TPEP** originates from HOMO−1 to LUMO. The calculated energy band gap between HOMO and LUMO of **TPEP** is 3.09 eV, but the agreement between the calculated and experimentally observed spectra is very poor (Supporting Information). It has been well documented in the literature that the B3LYP hybrid functional typically underestimates excitation energies in donor–acceptor complexes due to an incomplete cancellation of self-interaction effects. However, one can obtain better results implementing new, contemporary methods by using range-separated functionals for calculating excitation energies of D–A systems.[17]

Picric Acid Sensing. Among the NACs, PA[18] and TNT need considerable attention because of their highly explosive nature; consequently, detection of trace amounts of NACs has been a field of interest to researchers in recent years. NACs are main constituents in crackers, rocket fuels, and explosives.[19] Moreover, continuous terrorist activities all over the world have prompted the scientific community to design and synthesize efficient sensors for detecting explosives. Explosives are considered as the main soil contaminants in war-affected areas[20] and are also considered as health hazards.[21] Applications of nanoaggregates of the many organic molecules toward the sensing of explosives are well documented in the literature by Tang et al.,[22] Kumar et al.,[23] and others.[24] On the other hand, fluorescence-based detection takes advantage over other methods[25] due to its simple operation, time consumption, sensitivity, selectivity, and low cost.[26] In our previous work,[11b] we have reported the nanoaggregates of hydrazono-sulfonamide adducts as selective chemosensors for the detection of picric acid. In continuation of our studies, the highly emissive nature of fluorescent nanoaggregates of **TPEP** motivated us to screen its application as sensor for NACs. For fluorescence titration with NACs, we have utilized nanoaggregates of 90% water fraction. Incremental addition of PA to the nanoaggregates leads to a decrease in the emission intensity, and complete quenching was observed after addition of 40 equiv of picric acid (Figure 5a). We did not observe any change in wavelength during the addition of PA.

The data from fluorescence titrations were used to calculate the quenching constant using the Stern–Volmer equation (eq 1)

$$I_0/I = 1 + K_{SV}[Q] \quad (1)$$

where, I_0 and I are the PL intensities before and after addition of PA, [Q] is the quencher concentration, and K_{SV} is the Stern–Volmer or quenching constant.

The Stern–Volmer plot (I_0/I vs PA concentration) is presented in Figure 5b. At higher concentrations of PA, the plot bent upward due to super amplified quenching effect,[27] however, linearity at lower concentration PA indicates the involvement of static quenching mechanism. The quenching constant was found to be 5.6×10^5 M^{-1}. The turn-off mechanism is attributed to the electron transfer and/or energy transfer mechanism[28] between nanoaggregates of **TPEP** and picrate ion. The spectral overlap of the absorption spectrum of PA with the emission spectrum of **TPEP** in the wavelength region 424–494 nm promotes efficient energy transfer from the excited state of nanoaggregates of **TPEP** to the ground state of PA, thus further increasing the quenching efficiency. On the other hand, the electron-deficient nature of PA can easily quench the fluorescence of nanoaggregates of **TPEP** via an electron-transfer process. In addition to PA, we also screened other NACs such as 2,4,6-trinitrotoluene (TNT), 4-nitrobenzene (NB), 1,4-dintrophenol (DNP), and 4-nitrophenol (NP) for quenching of the fluorescence of nanoaggregates of **TPEP**; from the results, we conclude that the nanoaggregates of **TPEP** selectively and efficiently interact with PA than other NACs (Figure 6).

For practical usage, we have also demonstrated the test strip based detection of PA by using TLC plates. The fluorescent test strips were prepared using TLC plates coated by dipping into a solution of **TPEP**. The coated strips were dried under vacuum and then used for the solid-phase detection of PA. The highly emissive nature of the test strips becomes nonemissive when it is in contact with the PA (Figure 7). The detection limit was found to be in the range of 22 nM.[29]

■ CONCLUSION

In conclusion, tetraphenylethene–2-pyrone (**TPEP**) conjugate with donor–acceptor structure have been synthesized and structurally characterized. **TPEP** exhibits solvent polarity dependent photoluminescence characteristics, which confirm the involvement of the polar excited state in the emission process. This was further confirmed with theoretical TD-DFT calculations. **TPEP** is weakly emissive in dilute solutions and strongly emissive in the aggregated state. The detailed optical investigations revealed that restricted intermolecular rotation at

DOI: 10.1021/acs.joc.6b00267
J. Org. Chem. 2016, 81, 3597–3602

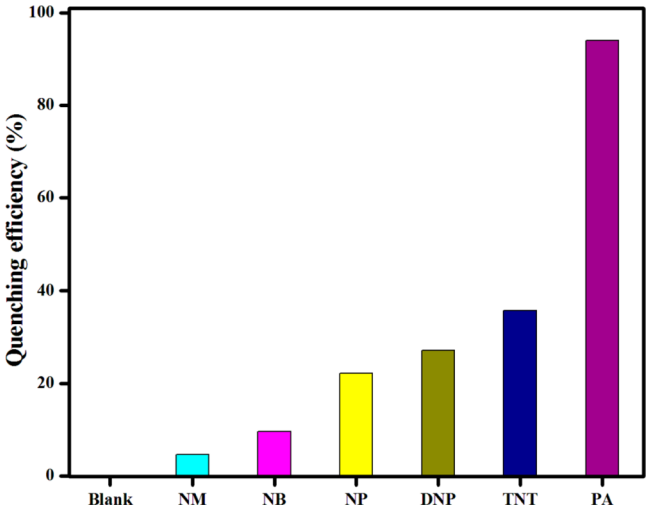

Figure 6. Relative fluorescence quenching of nanoaggregates of **TPEP** upon addition of various NACs (40 equiv) in THF/water (10:90) mixture.

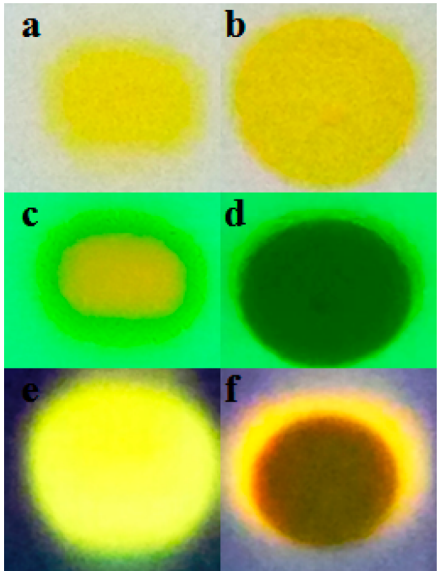

Figure 7. Test strips based detection of PA. Visualization of **TPEP** and **TPEP** with **PA** under day light (a, b), UV light 254 nm (c, d), and 365 nm (e, f).

the aggregated state is responsible for the aggregation-induced emission (AIE) characteristics. The luminescent nanoaggregates of **TPEP** were utilized for the selective detection and discrimination of explosive nitroaromatic compounds. In addition, low-cost fluorescent test strips for selective detection of PA were developed to show the merits of **TPEP**.

EXPERIMENTAL SECTION

Materials and Methods. Unless stated otherwise, all solvents and chemicals were obtained from commercial sources and used without further purification. Acetyl TPE[30] and SSA12[31] were prepared using the reported procedure, and spectral data are in good agreement with the literature. Analytical thin-layer chromatography (TLC) was performed on precoated silica gel-G plates using a mixture of petroleum ether (60−80 °C) and ethyl acetate (7:3) as the eluent. The NMR spectra were obtained at 300 MHz for ^{1}H and 75 MHz for ^{13}C using TMS as an internal standard and $CDCl_3$ as solvent. Chemical shifts are expressed in parts per million (ppm), and the coupling constants (J values) are expressed in hertz (Hz). The following abbreviations are used to indicate spin multiplicities: s (singlet), m (multiplet). Melting points were determined using open capillaries and are uncorrected. Absorption measurements were carried out on a single-beam UV-diode array spectrophotometer. Fluorescence emission studies were performed using a Fluoromax-4 spectrometer. Mass spectra were obtained with a Micromass Q-TOF mass spectrometer (ESI-HRMS). The morphological characterization of nanoaggregates was determined by using transmission electron microscopy. Single-crystal X-ray diffraction data were collected with a SMART APEX diffractometer equipped with a three-axis goniometer. Using Olex2, the structure was solved with the ShelXS structure solution program using direct methods and refined with the SHELXL refinement package using least squares minimization. The slit width was 5 nm for both excitation and emission. HPLC-grade solvents were used for photophysical measurements.

Preparation of Aggregates. A stock solution of **TPEP** was prepared in tetrahydrofuran (THF) (10^{-4} M). An aliquot (1 mL) of this stock solution was transferred to the volumetric flask. An appropriate amount of THF and water was added to the flask under vigorous stirring to obtain the 10^{-5} M THF/water mixture with water fractions of 0−90%. The spectral analysis of the resultant mixtures was measured immediately.

Caution! The nitroaromatic compounds used in this study, especially TNT and picric acid, are very powerful explosives. They must be handled with care and also in very small quantities.

Synthesis of TPEP. A mixture of acetyl TPE (4.4038 g, 0.0118 mol, 1.2 equiv), SSA (2.0000 g, 0.0098 mol, 1 equiv), and powdered potassium hydroxide (0.6599 g, 0.0118 mol, 1.2 equiv) in DMSO (8 mL) was stirred at room temperature for 13 h. The progress of the reaction was monitored by TLC, and on completion, the reaction mixture was poured into ice−water with constant stirring. The precipitate thus obtained was filtered and purified on silica gel column using petroleum ether/ethyl acetate as the eluent to afford TPEP (4.2 g, 87%) as a yellow solid: mp 230−232 °C; ^{1}H NMR (300 MHz, $CDCl_3$) δ 2.67 (s, 3H), 6.62 (s, 1H), 7.02−7.03 (m, 6H), 7.11−7.17 (m, 11H), 7.59−7.62 (d, J = 7.6, 2H); ^{13}C NMR (75 MHz, $CDCl_3$) δ 14.7, 90.3, 97.6, 113.4, 126.0, 126.9, 127.1, 127.3, 127.7, 127.9, 131.1, 131.2, 132.2, 139.3, 142.7, 142.9, 142.9, 143.2, 149.1, 157.2, 161.8, 169.7; HRESI-MS (m/z) calcd for $C_{33}H_{23}NO_2S$ (M + Na) 520.1347, found (M + Na) 520.1345.

ASSOCIATED CONTENT

Supporting Information

The Supporting Information is available free of charge on the ACS Publications website at DOI: 10.1021/acs.joc.6b00267.

Characterization data, spectral data, and crystal data for adduct **TPEP** and computational tables (PDF)

X-ray data for **TPEP** (CIF)

AUTHOR INFORMATION

Corresponding Author

*E-mail: shivazzen@mkuniversity.org.

Notes

The authors declare no competing financial interest.

ACKNOWLEDGMENTS

We thank DST and UGC for financial assistance and DST-IRHPA for funding the purchase of a higher resolution NMR spectrometer.

REFERENCES

(1) (a) Chou, T.-C.; Hwa, C.-L.; Lin, J.-J.; Liao, K.-C.; Tseng, J.-C. *J. Org. Chem.* **2005**, *70*, 9717. (b) Xu, Z.; Yoon, J.; Spring, D. R. *Chem. Soc. Rev.* **2010**, *39*, 1996.

DOI: 10.1021/acs.joc.6b00267
J. Org. Chem. 2016, 81, 3597−3602

(2) (a) Berezin, M. Y.; Achilefu, S. *Chem. Rev.* **2010**, *110*, 2641. (b) Meech, S. R. *Chem. Soc. Rev.* **2009**, *38*, 2922.
(3) (a) Goncalves, M. S. T. *Chem. Rev.* **2009**, *109*, 190. (b) Okamoto, A.; Kanatani, K.; Saito, I. *J. Am. Chem. Soc.* **2004**, *126*, 4820.
(4) (a) Wu, K.-C.; Ku, P.-J.; Lin, C.-S.; Shih, H.-T.; Wu, F.-I.; Huang, M.-J.; Lin, J.-J.; Chen, I.-C.; Cheng, C.-H. *Adv. Funct. Mater.* **2008**, *18*, 67. (b) Jia, W.-L.; McCormick, T.; Liu, Q.- D.; Fukutani, H.; Motala, M.; Wang, R.-Y.; Tao, Y.; Wang, S. *J. Mater. Chem.* **2004**, *14*, 3344. (c) Roncali, J. *Acc. Chem. Res.* **2000**, *33*, 147.
(5) (a) Luo, J.; Xie, Z.; Lam, J. W. Y.; Cheng, L.; Chen, H.; Qiu, C.; Kwok, H. S.; Zhan, X.; Liu, Y.; Zhu, D.; Tang, B. Z. *Chem. Commun.* **2001**, 1740. (b) Mei, J.; Hong, Y.; Lam, J. W. Y.; Qin, A.; Tang, Y.; Tang, B. Z. *Adv. Mater.* **2014**, *26*, 5429. (c) Mei, J.; Leung, N. L. C.; Lam, J. W. Y.; Tang, B. Z.; Kwok, R. T. K. *Chem. Rev.* **2015**, *115*, 11718.
(6) Hong, Y.; Lam, J. W. Y.; Tang, B. Z. *Chem. Commun.* **2009**, 4332.
(7) (a) Wang, E.; Zhao, E.; Hong, Y.; Lam, J. W. Y.; Tang, B. Z. *J. Mater. Chem. B* **2014**, *2*, 2013. (b) Sanji, T.; Shiraishi, K.; Nakamura, M.; Tanaka, M. *Chem. - Asian J.* **2010**, *5*, 817. (c) Kwok, R. T. K.; Leung, C. W. T.; Lam, J. W. Y.; Tang, B. Z. *Chem. Soc. Rev.* **2015**, *44*, 4228. (d) Wang, M.; Zhang, G.; Zhang, D.; Zhu, D.; Tang, B. Z. *J. Mater. Chem.* **2010**, *20*, 1858. (e) Zhao, Z.; Lam, J. W. Y.; Tang, B. Z. *J. Mater. Chem.* **2012**, *22*, 23726. (f) Tong, D.; Duan, H.; Wang, J.; Yang, Z.; Lin, Y. *Sens. Actuators, B* **2014**, *195*, 80.
(8) Yuan, W. Z.; Lu, P.; Chen, S.; Lam, J. W. Y.; Wang, Z.; Liu, Y.; Kwok, H. S.; Ma, Y.; Tang, B. Z. *Adv. Mater.* **2010**, *22*, 2159.
(9) (a) Zhao, Z.; Lam, J. W. Y.; Tang, B. Z. *J. Mater. Chem.* **2012**, *22*, 23726. (b) Ding, D.; Li, K.; Liu, B.; Tang, B. Z. *Acc. Chem. Res.* **2013**, *46*, 2441.
(10) (a) Chen, C. H.; Tang, C. W.; Shi, J.; Klubek, K. P. *Thin Solid Films* **2000**, *363*, 327. (b) Chen, C. H.; Tang, C. W.; Shi, J.; Klubek, K. P. *Macromol. Symp.* **1998**, *125*, 49.
(11) (a) Mahendran, V.; Shanmugam, S. *RSC Adv.* **2015**, *5*, 20003. (b) Mahendran, V.; Shanmugam, S. *RSC Adv.* **2015**, *5*, 92473.
(12) Tang, B. Z.; Geng, Y.; Lam, J. W. Y.; Li, B.; Jing, X.; Wang, X.; Wang, F.; Pakhomov, A. B.; Zhang, X. X. *Chem. Mater.* **1999**, *11*, 1581.
(13) Becke, A. D. *J. Chem. Phys.* **1993**, *98*, 5648.
(14) Frisch, M. J.; Trucks, G. W.; Schlegel, H. B.; Scuseria, G. E.; Robb, M. A.; Cheeseman, J. R.; Scalmani, G.; Barone, V.; Mennucci, B.; Petersson, G. A.; Nakatsuji, H.; Caricato, M.; Li, X.; Hratchian, H. P.; Izmaylov, A. F.; Bloino, J.; Zheng, G.; Sonnenberg, J. L.; Hada, M.; Ehara, M.; Toyota, K.; Fukuda, R.; Hasegawa, J.; Ishida, M.; Nakajima, T.; Honda, Y.; Kitao, O.; Nakai, H.; Vreven, T.; Montgomery, J. A., Jr.; Peralta, J. E.; Ogliaro, F.; Bearpark, M.; Heyd, J. J.; Brothers, E.; Kudin, K. N.; Staroverov, V. N.; Kobayashi, R.; Normand, J.; Raghavachari, K.; Rendell, A.; Burant, J. C.; Iyengar, S. S.; Tomasi, J.; Cossi, M.; Rega, N.; Millam, N. J.; Klene, M.; Knox, J. E.; Cross, J. B.; Bakken, V.; Adamo, C.; Jaramillo, J.; Gomperts, R.; Stratmann, R. E.; Yazyev, O.; Austin, A. J.; Cammi, R.; Pomelli, C.; Ochterski, J. W.; Martin, R. L.; Morokuma, K.; Zakrzewski, V. G.; Voth, G. A.; Salvador, P.; Dannenberg, J. J.; Dapprich, S.; Daniels, A. D.; Farkas, O.; Foresman, J. B.; Ortiz, J. V.; Cioslowski, J.; Fox, D. J. *Gaussian 09*, Revision C.01; Gaussian, Inc.: Wallingford, CT, 2010.
(15) Becke, A. D. *Phys. Rev. A: At., Mol., Opt. Phys.* **1988**, *38*, 3098.
(16) Lee, C.; Yang, W.; Parr, R. G. *Phys. Rev. B: Condens. Matter Mater. Phys.* **1988**, *37*, 785.
(17) Wong, B. M.; Piacenza, M.; Sala, F. D. *Phys. Chem. Chem. Phys.* **2009**, *11*, 4498 and references cited therein.
(18) *Safety Data Sheet for Picric Acid*, Resource of UK National Institute of Health, London.
(19) Akhavan, J. *The Chemistry of Explosives*; Royal Society of Chemistry, 2011.
(20) Shanmugaraju, S.; Joshi, S. A.; Mukherjee, P. S. *J. Mater. Chem.* **2011**, *21*, 9130.
(21) Ashbrook, P. C.; Houts, T. A. *Chem. Health Saf.* **2003**, *10*, 27.
(22) (a) Chan, C. Y. K.; Zhao, Z.; Lam, J. W. Y.; Liu, J.; Chen, S.; Lu, P.; Mahtab, F.; Chen, X.; Sung, H. H. Y.; Kwok, H. S.; Ma, Y.; Williams, I. D.; Wong, K. S.; Tang, B. Z. *Adv. Funct. Mater.* **2012**, *22*, 378. (b) Zhang, Y.; Chen, G.; Lin, Y.; Zhao, L.; Yuan, W. Z.; Lu, P.; Jim, C. K. W.; Zhang, Y.; Tang, B. Z. *Polym. Chem.* **2015**, *6*, 97. (c) Li, H.; Wu, H.; Zhao, E.; Li, J.; Sun, J. Z.; Qin, A.; Tang, B. Z. *Macromolecules* **2013**, *46*, 3907.
(23) (a) Kaur, S.; Bhalla, V.; Vij, V.; Kumar, M. *J. Mater. Chem. C* **2014**, *2*, 3936. (b) Pramanik, S.; Bhalla, V.; Kumar, M. *Anal. Chim. Acta* **2013**, *793*, 99. (c) Vij, V.; Bhalla, V.; Kumar, M. *ACS Appl. Mater. Interfaces* **2013**, *5*, 5373.
(24) Sathish, V.; Ramdass, A.; Lu, Z.−Z.; Velayudham, M.; Thanasekaran, P.; Lu, K.−L.; Rajagopal, S. *J. Phys. Chem. B* **2013**, *117*, 14358.
(25) (a) Zu, B.; Guo, Y.; Dou, X. *Nanoscale* **2013**, *5*, 10693. (b) Sylvia, J.; Janni, J.; Klein, J.; Spencer, K. *Anal. Chem.* **2000**, *72*, 5834. (c) Wallenborg, S.; Bailey, C. *Anal. Chem.* **2000**, *72*, 1872.
(26) (a) Hodyss, R.; Beauchamp, J. L. *Anal. Chem.* **2005**, *77*, 3607. (b) Moore, D. S. *Rev. Sci. Instrum.* **2004**, *75*, 2499. (c) Riskin, M.; Tel-Vered, R.; Bourenko, T.; Granot, E.; Willner, I. *J. Am. Chem. Soc.* **2008**, *130*, 9726.
(27) Li, D.; Liu, J.; Kwok, R. T. K.; Liang, Z.; Tang, B. Z.; Yu, J. *Chem. Commun.* **2012**, *48*, 7167.
(28) Ma, J.; Lin, T.; Pan, X.; Wang, W. *Chem. Mater.* **2014**, *26*, 4221.
(29) Venkatesan, N.; Singh, V.; Rajakumar, P.; Mishra, A. K. *RSC Adv.* **2014**, *4*, 53484.
(30) Wolf, M. O.; Fox, H. H.; Fox, M. A. *J. Org. Chem.* **1996**, *61*, 287.
(31) (a) Tominaga, Y.; Ushirogochi, A.; Matsuda, Y. *J. Heterocycl. Chem.* **1987**, *24*, 1557. (b) Tominaga, Y.; Ushirogochi, A.; Matsuda, Y.; Kobayashi, G. *Chem. Pharm. Bull.* **1984**, *32*, 3384.

DOI: 10.1021/acs.joc.6b00267
J. Org. Chem. 2016, 81, 3597−3602